Proceedings of the 2005 IEEE
Engineering in Medicine and Biology 27th Annual Conference
Shanghai, China, September 1-4, 2005

An Improved Electronic Colon Cleansing Method for Detection of Polyps by Virtual Colonoscopy

Zigang Wang[1], Xiang Li[1,2], Lihong Li[1,3], Bin Li[1], Daria Eremina[4], Hongbing Lu[5], and Zhengrong Liang[1,6,7]

Departments of Radiology[1], Applied Mathematics and Statistics[4], Computer Science[6], and Physics and Astronomy[7], State University of New York, Stony Brook, NY, USA

Department of Radiation Oncology[2], Columbia University, New York, NY, USA

Department of Engineering Science and Physics[3], City College of Staten Island of the City University of New York, New York, NY, USA

Department of Computer Application/BME[5], the Fourth Military Medical University, Xi'an, Shaanxi 710032, China

Abstract - **Electronic colon cleansing (ECC) aims to segment the colon lumen from the patient abdominal image acquired with colonic material tagging by oral contrast and other means, so that a virtual colon model can be constructed. Virtual colonoscopy (VC) navigates through the colon model looking for polyps in a similar manner as the fiber optic colonoscopy does. We had built an ECC pipeline for the commercial VC system of Viatronix Inc. In this paper, we present an improved ECC method. It is based on a partial-volume image-segmentation framework, which is derived using the well-established statistical expectation-maximization algorithm. The presented ECC method was evaluated by both visual inspection on the cleansed colon lumens and computer-aided detection of polyps (CADpolyp) using 20 patient datasets. Compared to our previous ECC pipeline, this presented new method demonstrates improvement in both visual judgment and CADpolyp.**

1 INTRODUCTION

Colon cancer is the third most common human malignancy and the second leading cause of cancer-related deaths in the United States in 2004 [1]. It results in more than 130,000 new cases and 56,000 deaths each year. The overall risk of developing the disease is approximately 5% over a lifetime. More than 90% colon cancer is developed from adenomatous polyps, which take five to 15 years for malignant transformation. Early detection and removal of the polyps will dramatically reduce the risk of the death [2]. Currently available detection methods consist of fecal occult blood test, sigmoidoscopy, barium enema, and fiber optic colonoscopy (OC), where OC is currently the gold standard. Virtual colonoscopy (VC) is an emerging method for the detection of polyps. VC utilizes advanced medical imaging and computer technologies to mimic the OC procedure, looking for polyps by navigating through a virtual colon model which is constructed from the patient abdominal images [3]. Compared to OC, VC has shown the potential to become a mass screening modality in terms of safety, cost, and patient compliance [4]. Thus the positive findings by VC screening would be examined by OC follow-up [5].

We have been developing VC as a screening modality using computed tomography (CT) technologies [3, 6]. Firstly, the patient undergoes a less-stressful bowel preparation with oral contrast to tag the colonic material, so that the residue stool and fluid have an enhanced CT image density. Then electronic colon cleansing (ECC) is performed by image segmentation of the air and enhanced material inside the colon lumen. A virtual model of the cleansed lumen is then constructed. To facilitate navigation through the entire colon lumen model, a centerline and its associated fly-through potential field are built within the lumen space. Three-dimensional (3D) endoscopic views are generated by prospective volume rendering of the colon wall in a nearly real-time fashion when navigating through the potential field on a PC platform. Interactive toolsets are available with translucent views for "electronic biopsy" on suspicious areas on the wall. A prototype integrating our previously-developed components along the above research track was licensed to Viatronix Inc. to build the FDA-approved commercial V3D-Colon Module (visualization and navigation system). A multi-center clinical trial on 1,233 asymptomatic patients using this commercial VC system has shown a comparable detection of clinically significant polyps as OC does [4]. This work presents an improved ECC method as compared to that in the prototype.

The content of this paper is organized as follows. Section 2 presents the improved ECC method. Validation of the method by 20 patient datasets is reported in Section 3, followed by discussion and conclusion in Section 4.

2 METHODS

The ECC method to be presented is based on the following partial volume (PV) image segmentation framework.

2.1. Partial Volume Image Segmentation Algorithm

Let the acquired CT image density distribution Y be represented by a column vector $[y_1, y_2, ..., y_N]^T$, where y_i is the observed density value at voxel i, N is the total number of voxels in the image. Assume the acquired image $\{y_i\}$ contains K tissue types distributing inside the body. Within each voxel i, there possibly are K tissue types, where each tissue type has a contribution to the observed density value y_i at that voxel. Let tissue type k contributes x_{ik} to the observation y_i at voxel i, then we have $y_i = \sum_{k=1}^{K} x_{ik}$.

Assume the unobservable variable x_{ik} follows a Gaussian distribution with mean μ_{ik} and variance σ_{ik}^2. If voxel i is fully filled by tissue type k, then x_{ik} becomes observable variable, *i.e.*, y_i in this case, with Gaussian probability distribution characterized by tissue parameters (μ_k and σ_k^2). If voxel i is partially filled by tissue type k and let m_{ik} be the fraction of tissue type k inside that voxel, then we have $\mu_{ik} = m_{ik}\mu_k$ and $\sigma_{ik}^2 = m_{ik}\sigma_k^2$, where $\sum_{k=1}^{K} m_{ik} = 1$, $0 \le m_{ik} \le 1$ and $(\mu_k, \sigma_k^2, \mu_{ik}, \sigma_{ik}^2) \ge 0$.

By the definitions above and the use of the EM algorithm [7], our partial volume image segmentation algorithm is [8]:

$$\mu_k^{(n+1)} = \frac{\sum_{i=1}^{N} x_{ik}^{(n)}}{\sum_{i=1}^{N} m_{ik}^{(n)}}. \tag{1}$$

$$\sigma_k^{2(n+1)} = \frac{1}{N}\sum_{i=1}^{N} \frac{x_{ik}^{2(n)} - 2m_{ik}^{(n)}\mu_k^{(n)}x_{ik}^{(n)} + m_{ik}^{2(n)}\mu_k^{2(n)}}{m_{ik}^{2(n)}} \tag{2}$$

$$m_{i1}^{(n+1)} = \frac{x_{i1}^{(n)}\sigma_{i2}^{2(n)}\mu_1^{(n)} + \sigma_{i1}^{2(n)}\mu_2^{2(n)} - x_{i2}^{(n)}\sigma_{i1}^{2(n)}\mu_2^{(n)} + 4\beta\sigma_{i1}^{2(n)}\sigma_{i2}^{2(n)}\sum_{j\in N_i}\alpha_{ij}m_{j1}^{(n)}}{\mu_1^{2(n)}\sigma_{i2}^{2(n)} + \mu_2^{2(n)}\sigma_{i1}^{2(n)} + 4\beta\sigma_{i1}^{2(n)}\sigma_{i2}^{2(n)}\sum_{j\in N_i}\alpha_{ij}} \tag{3}$$

$$\begin{aligned} x_{ik}^{(n)} &= \mathrm{E}[x_{ik} \mid y_i, M^{(n)}, \mu^{(n)}, \sigma^{2(n)}] \\ &= m_{ik}^{(n)}\mu_k^{(n)} + \frac{m_{ik}^{2(n)}\sigma_k^{2(n)}}{\sum_{j=1}^{K} m_{ij}^{2(n)}\sigma_j^{2(n)}} \cdot \left(y_i - \sum_{j=1}^{K} m_{ij}^{(n)}\mu_j^{(n)}\right) \end{aligned} \tag{4}$$

$$\begin{aligned} x_{ik}^{2(n)} &= \mathrm{E}[x_{ik}^2 \mid y_i, M^{(n)}, \mu^{(n)}, \sigma^{2(n)}] \\ &= (x_{ik}^{(n)})^2 + m_{ik}^{2(n)}\sigma_k^{2(n)} \frac{\sum_{j\neq k}^{K} m_{ij}^{2(n)}\sigma_j^{2(n)}}{\sum_{j=1}^{K} m_{ij}^{2(n)}\sigma_j^{2(n)}}. \end{aligned} \tag{5}$$

where N_i denotes the neighborhood of voxel i, β is a parameter controlling the degree of the penalty on the mixture M, and α_{ij} is a scale factor reflecting the difference among different orders of the neighbors.

Equations (1)-(5) provide a pML or MAP-EM solution for the PV image segmentation under the constraint that each voxel has a maximum of two tissue types. There is no limitation on how many tissue types in the image. In our case, the CT image may contain four tissue types with different image densities, *i.e.*, K = 4: (1) air in the colon lumen and lungs, (2) fat or soft tissues, (3) muscle, and (4) bone or tagged colonic material. This known information can be utilized to facilitate the segmentation of a CT image into mixtures of maximum two tissue types in each voxel.

2.2. Cleansing the Colon Lumen and Extracting the Mucosa Layer

After the PV image segmentation, the voxels in the colon lumen are classified as air, mixture of air with tissue, mixture of air with tagged material, and mixture of tissue with tagged material. A region growing strategy is applied to connect those voxels of air and mixture of air with tagged colonic material for the colon lumen space. The mixtures of tissue with air and tissue with tagged material are extracted for the mucosa layer.

Given a cleansed colon lumen, the Viatronix V3D-Colon Module is used to construct the corresponding virtual colon model and navigate through the colon lumen, examining the colon wall by the volume-rendered 3D endoscopic views. The quality of the 3D endoscopic views from the presented ECC method is compared to that of our previous ECC pipeline by the users' visual judgment.

Given an extracted mucosa layer, our previously developed surface-based [9] and texture-based [10] CAD techniques are used to analyze the extracted mucosa layer for polyp detection. The CADpolyp result from this presented ECC method is compared to that of our previous ECC pipeline.

3. RESULTS

Twenty patients' CT datasets were used to evaluate the efficiency of the presented ECC method with comparison to our previously developed ECC pipeline in the commercial V3D-Colon Module. These datasets were acquired from patients who followed a less-stressful bowel preparation with low-residue diet and oral contrast tagging of the colonic material [5]. A single-slice spiral CT scanner was used with clinically available protocols to cover the entire abdominal volume during a single breath-holding acquisition time period. Each patient study included both supine and prone scans (resulting in a total of 40 scans). The detector collimation was 5 mm and the images were reconstructed as 1mm thickness of 512×512 arrays. Among these 20 patient datasets, nine contained at least one colon polyp larger than 5 mm in diameter. These polyp sizes and their positions were documented by OC and verified by radiologists' VC navigation through the colon models.

These datasets were first processed by our previous ECC pipeline and then processed by this presented ECC method. The cleansed colon lumens were input to the V3D-Colon Module for construction of virtual colon model and inspection via fly-through navigation.

In our previous ECC pipeline, the image segmentation was performed first by a hard segmentation [5], followed by an improvement by a soft segmentation [11] which determines the probability of a tissue type or label falling into a voxel and does not compute directly the mixtures $\{m_{ik}\}$. Removal of the voxels of tagged colonic material was based on a ray-tracing strategy [12], which starts at an air voxel selected inside the colon lumen and detects the boundaries between the air and the tagged material and between the tagged material and the colon wall.

By fly-through all the virtual colon models, the presented ECC method show an improvement over our previous ECC pipeline by visual inspection. Figure 1 shows an example which compares this current image segmentation method with our previous one.

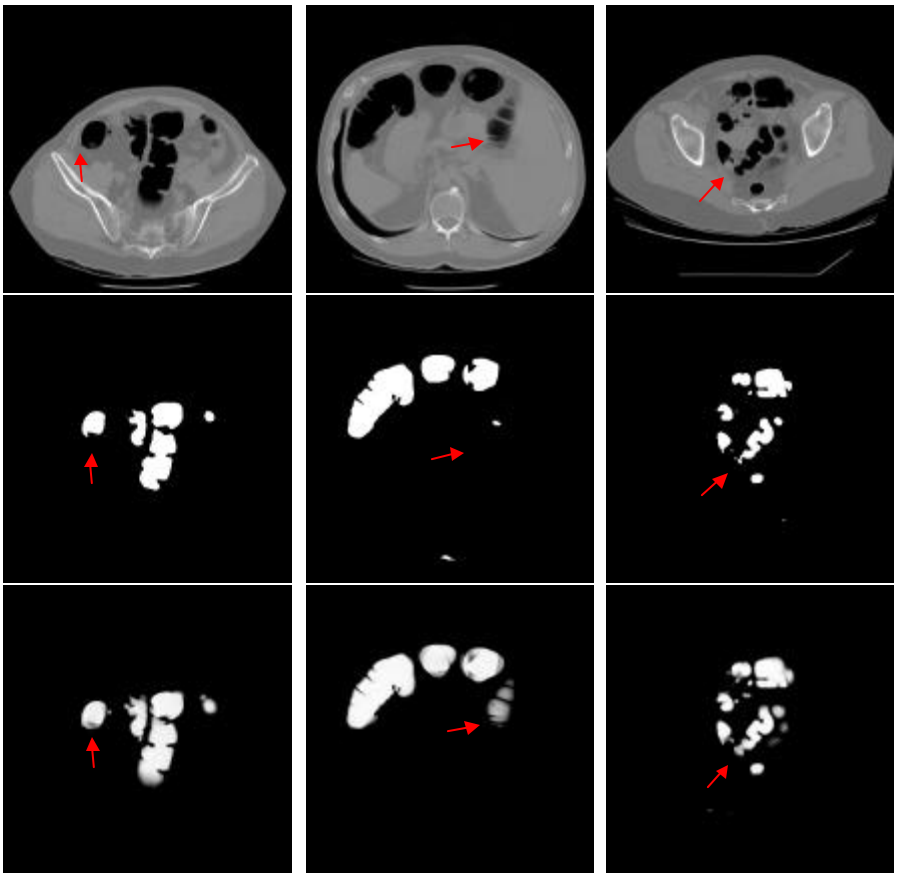

Figure 1. Comparison of two different image segmentation methods. The images in the top row are the original CT images. The middle row shows the results of our previous segmentation algorithm. The results of our current segmentation method are shown in the bottom row.

The presented PV image segmentation preserves more details (see the bottom row of Figure 1) than our previous hard/soft image segmentation does (see the middle row). A small polyp, indicated by the red arrows in the middle column, is retained in the segmentation of our current method and disappears in the segmentation of our previous algorithm. In the right column, the shape of a polyp, indicated by the red arrows, is well preserved in the segmentation of the current method and is altered in the segmentation of the previous algorithm. Their difference can also be seen from their performance of removing the tagged colonic material. An example is shown by Figure 2. The presented ECC method shows an improvement for the lumen cleansing, see the results in the right column. Since the current method cleanses the lumen based on the PV image segmentation and the bone and tagged colonic material can not be distinguished in the segmentation, therefore, the bone is also removed. In our previous cleansing pipeline, we start the process from a selected voxel inside the lumen and, therefore, the bone outside the lumen is preserved. The bone outside the lumen has no effect on the fly-though navigation inside the lumen and on the performance of the CADpolyp.

In addition to the above visual judgment, we also performed CADpolyp on the cleansed colons of the two ECC methods. A surface- or geometry-based CAD approach [9] was used first. It combines both the traditional local principal curvature measures and a modified or smoothed version (which is called global principal curvature measures) to quantify the shape of the extracted mucosa layers from the segmentations of our previous and current methods. The results are shown in Table 1. In addition to the surface-based CAD, we also applied our texture-based CAD to the cleansed colons [10]. This texture-based CAD utilizes additional morphological and texture information of the detected suspect to reduce the false positives. Since the same CAD parameters were used for both the ECC methods, the sensitivity and the false-positive rate per dataset shall reflect the difference among these two different ECC methods. For 100% detection sensitivity, both the CADpolyp schemes show improvement by the presented ECC method.

4. Discussion and Conclusion

An improved ECC method was presented with evaluation by 20 patient studies. The improvement was shown by both visual judgment on the segmented/cleansed colons and quantitative measures using CADpolyp means. The improvement is mainly due to the PV image segmentation which preserves more details than our previous hard/soft segmentation does.

The presented PV image segmentation is fully within the EM framework which maximizes the conditional expectation of the underline tissue process given the acquired data, different from the previous approaches [13] which maximize directly the probability likelihood of the acquired incomplete-data. A through comparison between this EM framework and the previous approaches is needed to show their difference.

The PV image model of this presentation would be the consequence of the discrete PV model of [14] when the discrete down-sampling is performed infinite times and the number of labels becomes infinite. A through comparison between this continuous PV model and the discrete PV model [14] is an interesting topic and is currently under progress.

Both this PV presentation and the previous work [14] share the same view of constraining the maximum number of tissue types in each voxel to be two, even the single image can have more than two tissue types. Use of the known tissue types may be helpful to improve the segmentation of more than

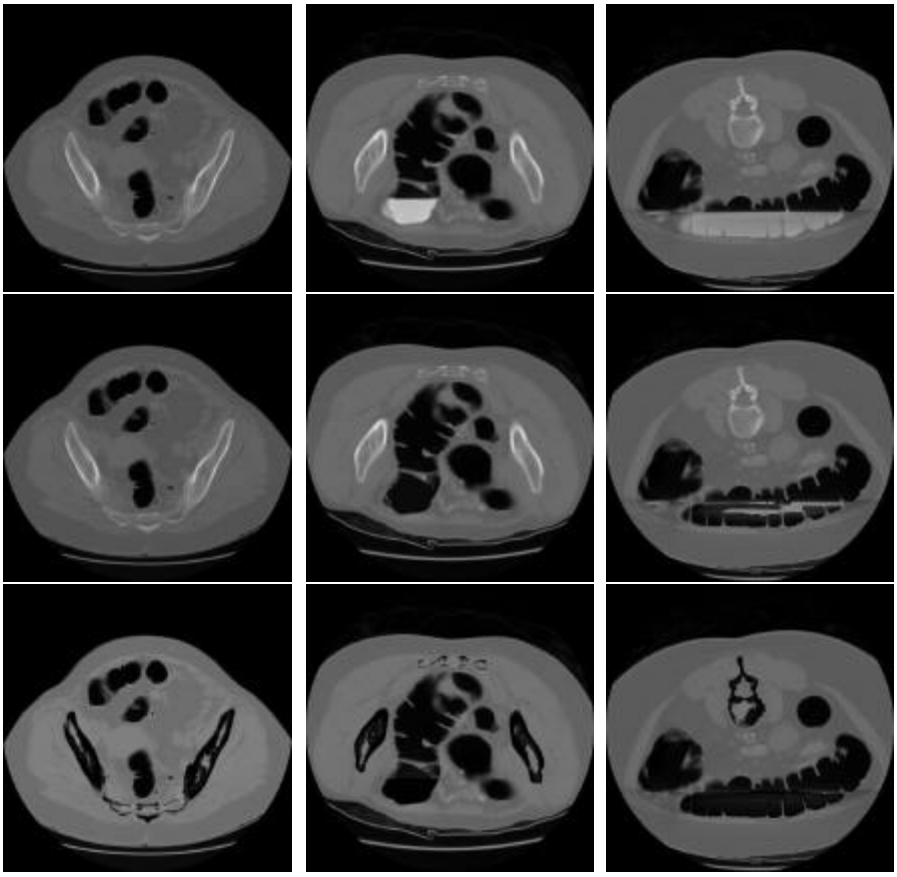

Figure 2: Comparison of two different cleansing methods. The images at the top row are the original CT images. The results by our previous cleansing pipeline are shown in the middle row. The results by this presented cleansing method are shown at the bottom row.

two tissue types in a voxel from a single image [15]. In our opinion, use of multispectral images is a more statistically-robust approach. This is a case in segmentation of magnetic resonance images of T_1-, T_2-, proton density-weighted scans [8]. By these three images, we can determine statistical-reliably four tissue types inside a voxel.

In the derivation of the close form of equation (3), we assumed the variance is fixed at the n-th iteration. This assumption [15] results in a quadratic form for the conditional expectation and makes its maximization (or minimization if the minor sign is changed to plus) numerically tractable. However, its effect on the EM iterative convergence needs to be proved.

	Shape-based CAD (Sensitivity~FP Rate)	Texture-based CAD (Sensitivity~FP Rate)
Previous ECC	100%~153.7/per dataset	100%~2.19/per dataset
Current ECC	100%~147.7/per dataset	100%~2.06/per dataset

Table 1. Comparison of CADpolyp on the virtual colons cleansed by two different ECC methods.

ACKNOWLEDGMENTS

This work was partly supported by NIH Grant #CA082402 and #CA110186 of the National Cancer Institute. The authors would like to acknowledge the use of the Viatronix V3D-Colon Module (or VC visualization and navigation system).

REFERENCES

[1] "Cancer Facts & Figures 2004", *American Cancer Society Annual Report*, 2004.

[2] M. O'Brien, S. Winawer, A. Zauber, L. Gottlieb, S. Sternberg, B. Diaz, G. Dickersin, S. Ewing, S. Geller, and D. Kasimian, "The national polyp study: patient and polyp characteristics associated with high-grade dysplasia in colorectal adenomas", *Gastroenterology*, **98**:371-379, 1990.

[3] L. Hong, A. Kaufman, Y. Wei, A. Viswambharan, M. Wax, and Z. Liang, "3D virtual colonoscopy", *IEEE Symposium on Frontier in Biomedical Visualization*, IEEE CS Press, pp. 26-32, 1995.

[4] P. Pickharder, J. Choi, I. Hwang, J. Butler, M. Puckett, H. Hildebrandt, R. Wong, P. Nugent, P. Mysliwiec, and W. Schindler, "Computed tomographic virtual colonoscopy to screen for colorectal neoplasia in asymptomatic adults", *New England Journal of Medicine*, **349**: 2191-2200, 2003.

[5] Z. Liang, S. Lakare, M. Wax, D. Chen, J. Anderson, A. Kaufman, and D. Harrington, "A pilot study on less-stressful bowel preparation for virtual colonoscopy screening with follow-up biopsy by optical colonoscopy", *SPIE Medical Imaging*, **5746**: 810-816, 2005.

[6] Z. Liang, "Virtual colonoscopy: an alternative approach to examination of the entire colon", *INNERVISION*, **16**: 40-44, 2001.

[7] A. Dempster, N. Laird, and D. Rubin, "Maximum likelihood from incomplete data via the EM algorithm," *Journal of Royal Statistical Society*, **39**: 1-38, 1977.

[8] Z. Liang, X. Li, D. Eremina, and L. Li, "An EM framework for segmentation of tissue mixtures from medical images", *Intl. Conf. of IEEE Engineering in Medicine and Biology*, Concun, Mexico, pp. 682-685, 2003.

[9] Z. Wang, L. Li, and Z. Liang, "Skeleton-based 3D computer aided diagnosis for detection of colonic polyps", *SPIE Medical Imaging*, **5032**: 843-853, 2003.

[10] Z. Wang, L. Li, J. Anderson, D. Harrington and Z. Liang, "Computer aided detection and diagnosis of colon polyps with morphological and texture features", *SPIE Medical Imaging*, **5370**: 972-979, 2004.

[11] L. Li, D. Chen, S. Lakare, K. Kreeger, I. Bitter, A. Kaufman, M. Wax, P. Djuric, and Z. Liang, "An image segmentation approach to extract colon lumen through colonic material tagging and hidden Markov random field model for virtual volonoscopy", *SPIE Medical Imaging*, **4683**: 406-411, 2002.

[12] S. Lakare, D. Chen, L. Li, A. Kaufman, and Z. Liang, "Electronic colon cleansing using segmentation rays for virtual colonoscopy", *SPIE Medical Imaging*, **4683**: 412-418, 2002.

[13] H. Choi, D. Haynor, and Y. Kim, "Partial volume tissue classification of multichannel magnetic resonance images – a mixel model", *IEEE Transactions on Medical Imaging* vol. 10, no. 2, pp. 395-407, 1991.

[14] K. Van. Leemput, F. Maes, D. Vandermeulen, and P. Suetens, "A unifying framework for partial volume segmentation of brain MR images," *IEEE Transactions on Medical Imaging*, **22**: 105-119, 2003.

[15] X. Li, Z. Liang, P. Zhang, and G. Kutcher, "An accurate colon residue detection algorithm with partial volume segmentation", *SPIE Medical Imaging*, **5370**: 1419-1426, 2004.